Journal of Fluids and Structures (2001) **15,** 1089–1102
doi:10.1006/jfls.2001.0386, available online at http://www.idealibrary.com on IDEAL®

AN APPLICATION OF FEEDBACK CONTROL TO STABILISE A SPECIFIC CASE OF THE NEGATIVE BUOYANCY FLOW INSTABILITY

J. E. Ffowcs Williams and A. S. Morgans

Department of Engineering, University of Cambridge Trumpington Street Cambridge CB2 1PZ, U.K.

(Received 1 February 2001, and in final form 19 April 2001)

This paper is one that David Maull would have enjoyed savaging. Firstly, because he always enjoyed lively discussions about hare-brained schemes for using feedback control to produce unnatural states of motion, and secondly, because he was never happier than when probing details of imaginative undergraduate projects. This paper results from such a project in the group where David spent most of his professional life, a project so far-fetched that it would have attracted his most critical attention. It would also have attracted his characteristically encouraging support.

The idea that instabilities of inviscid vortex sheets, which prevent them from being naturally steady, might be controlled through suitably excited actuators is being tentatively advanced, and some peculiar features of the controlled state also attract attention. The project that produced this paper addressed one peculiarity that turned out to be an error [see Ffowcs Williams (1982)], the solution to the actively controlled sheet turning out to be different and much simpler; this solution is published in Ffowcs Williams (2001). The project went on to consider whether another planar interface that is naturally unstable might be made stable by the action of an adjustable nearby surface. The situation envisaged is an unstable density stratified arrangement where heavy fluid lies initially at rest above a lighter fluid, the interface between the two fluids being planar. Above the interface is an impervious structural surface, which can be moved by a small amount by actuators designed to induce in the fluid a motion that will prevent the growth of any gravitational mode of instability. We show that it is indeed possible to define a controller with the required performance, but its implementation would be a very demanding task. A finite body of fluid could, on the other hand, be held suspended against gravity by relatively straightforward control arrangements. A particular example is worked out in detail and the control actuators defined, as is the transfer function between small oscillations of the interface and the actuator that is needed to implement the control system. An example is given to show how the unstable (but controlled) interface wobbles but settles down to rest after suffering an externally induced disturbance.

1. INTRODUCTION

The early stages of flow instability that eventually lead to unsteadiness can be modelled using linear theory. This is based on the idea that all disturbances are infinitesimally small at birth; small disturbances are linear and hence their behaviour can be described by linearising the equations of fluid motion about the steady solution.

Active control might sometimes be used to prevent the growth of disturbances in a naturally unstable flow. The control system would be coupled to the original flow system, and be designed, based on a linear model of the flow, so that the coupled system became stable. Disturbances would then never grow to such amplitudes that results in the

0889–9746/01/071089 + 14 $35.00/0

breakdown of the steady flow. Peak & Crighton (2000) have recently summarised this topic, and given examples of flow instabilities calmed by linear controllers.

This paper considers two specific cases of the negative buoyancy instability, featuring two-dimensional motion in a body of water suspended on the underside of a ceiling. The first case is the unbounded layer of water and the second a layer confined between two vertical walls. Surface tension exists, and the extent of the confined layer in the second example is such that only one wavelength is gravitationally unstable. It is shown that it is possible to stabilise these systems using active control, and that the control system required for the single mode example is both simple and realisable. This means that the seemingly unnatural state of maintaining water on the underside of a ceiling indefinitely is in fact both possible and feasible.

The purpose of the paper is not to put forward a serious proposal for keeping water on the ceiling, but rather to demonstrate for simple cases that active control techniques really can be used to prevent instabilities occurring in naturally unstable continuous systems. In doing so, they can dramatically change the natural properties of the system.

2. THE UNBOUNDED LAYER

The unbounded system consists of a layer of water suspended underneath a ceiling in a gravitational field. Below the water there is air whose density is assumed to be negligible compared to that of the water. The interface has constant surface tension T per unit depth into the page. It is assumed that the water is incompressible and inviscid. Although the density change across the interface will generate vorticity, the inviscid assumption means that the vorticity cannot diffuse away from the interface and the water remains irrotational. Figure 1 gives a schematic of the problem.

Since water is denser than air, the negative buoyancy instability may occur. In order to investigate the idea that it is possible to use an active controller to inhibit this instability, a highly idealised form of active control is considered. It is assumed that the upper surface at $y = H$ can deform into a shape $\varepsilon(x, t)$, and that a linear controller makes $\varepsilon(x, t)$ a linear function of the interface displacement. It is thereby assumed that the space–time Fourier transform of the displacement of this upper surface, $\hat{\varepsilon}(k, \omega)$, can be made to be some function, $Z(k, \omega)$, multiplied by the space–time Fourier transform of the interface displacement, $\hat{\eta}(k, \omega)$. That is, we get

$$\hat{\varepsilon}(k, \omega) = Z(k, \omega)\,\hat{\eta}(k, \omega). \tag{1}$$

2.1. Determining the Stability of the System

A flow is spatially unstable if a localised disturbance grows as it develops in space and is temporally unstable if an initial disturbance grows as time progresses. For most real flows, time and space are strongly coupled and there is a strong interrelation between spatial and temporal instability.

The interface displacement, $\eta(x, t)$, can be written in terms of its Fourier transform as

$$\eta(x, t) = \frac{1}{4\pi^2} \int_{-\infty}^{\infty} \int_{-\infty}^{\infty} \hat{\eta}(k, \omega) \mathrm{e}^{\mathrm{i}kx} \mathrm{e}^{\mathrm{i}\omega t}\, \mathrm{d}k\, \mathrm{d}\omega. \tag{2}$$

The displacement $\eta(x, t)$ is thus decomposed into Fourier elements in space and time. A single element of wavenumber k and frequency ω is an elementary wave:

$$\hat{\eta}(k, \omega)\mathrm{e}^{\mathrm{i}kx}\mathrm{e}^{\mathrm{i}\omega t} = \hat{\eta}(k, \omega)\mathrm{e}^{\mathrm{i}k(x + \omega t/k)} = \hat{\eta}(k, \omega)\mathrm{e}^{\mathrm{i}k(x - ct)}.$$

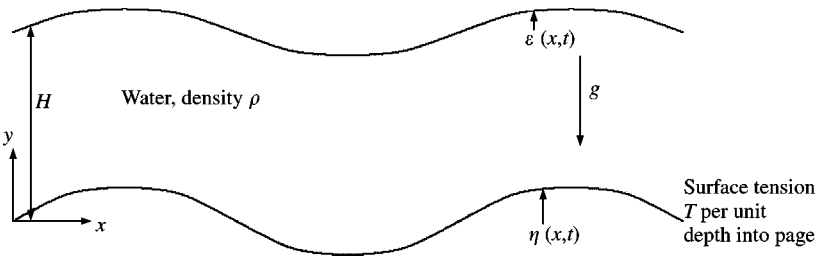

Figure 1. The unbounded layer of water.

It has constant phase on trajectories $x = ct$, where c is the wave/phase speed and is given by $c = -\omega/k$.

To investigate the spatial stability of the system, it is assumed that the disturbance is localised and is periodic in time. This means that ω is real. From equation (2) it can be seen that if the wave speed, c, has an imaginary component, there can be an exponentially increasing term inside the integral. This represents the disturbance growing with distance, and thus means that the system is spatially unstable. Similarly, to investigate temporal stability, it is assumed that an initial disturbance that is periodic in space occurs. This means that k is real. Again, if the wave speed, c, has an imaginary component, it can be seen from equation (2) that there can be an exponentially increasing term inside the integral, which represents growth of the disturbance as it develops in time. Thus, if the wave speed has an imaginary component, the system can be, and in fact is, temporally unstable.

So, the system in Figure 1 is both temporally and spatially unstable if the wave speed, $c = -\omega/k$, has an imaginary component of the right sign. The aim of the active control is to ensure that the wave speed becomes entirely real, since this ensures that instability does not occur.

2.2. Analysis

The flow in the water region is incompressible, inviscid and irrotational, and therefore obeys Laplace's equation and the unsteady Bernoulli equation,

$$\frac{\partial^2\phi}{\partial x^2} + \frac{\partial^2\phi}{\partial y^2} = 0, \tag{3}$$

$$p + \rho\frac{\partial\phi}{\partial t} + \rho g y + \frac{1}{2}\rho|\boldsymbol{v}|^2 = \text{constant}. \tag{4}$$

Force equilibrium at the interface relates the pressure difference to the capillary force,

$$\hat{\bar{p}}_2 - \hat{\bar{p}}_1 + (Tk^2 - \omega^2 m)\hat{\eta} = 0. \tag{5}$$

The boundary conditions for velocity are

$$\begin{aligned} &\frac{\partial\phi}{\partial y} = \frac{\partial\varepsilon}{\partial t} \quad \text{at } y = H + \varepsilon(x,t) \ (\varepsilon \text{ small});\\ &\frac{\partial\phi}{\partial y} = \frac{\partial\eta}{\partial t} \quad \text{at } y = \eta \ (\eta \text{ small}). \end{aligned} \tag{6}$$

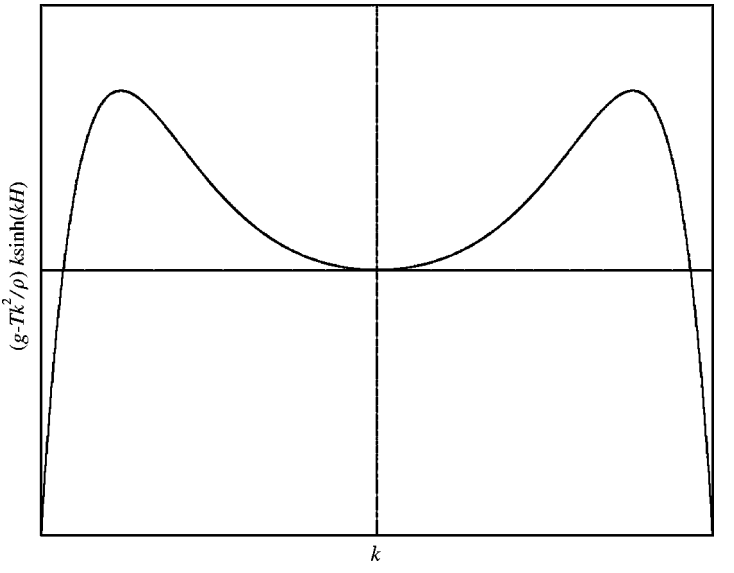

Figure 2. A plot of $(g - Tk^2/\rho)k\sinh(kH)$ against k.

Combining equation (3) to equation (5) and applying equation (6) gives the following expression for the wave speed ($c = -\omega/k$),

$$c^2\left(\rho k\left(\frac{1}{\tanh(kH)} - \frac{Z(k,\omega)}{\sinh(kH)}\right)\right) + \rho g - Tk^2 = 0. \tag{7}$$

It is not possible to solve this equation for c without assuming more about the form of $Z(k, \omega)$. This is because Z, by nature of being a function of k and ω, is also a function of c.

2.3. Identifying a Controller

If a simple trial function for Z is chosen to be $Z = A/\omega^2$, where A is a constant, it is found that the expression for the wave speed becomes

$$c^2\left(\frac{\rho k}{\tanh(kH)}\right) + \rho g - Tk^2 - \frac{\rho A}{\sinh(kH)} = 0. \tag{8}$$

The c^2 coefficient is always positive which means that the requirement for stability is that $\mathrm{Im}(A) = 0$ and $\mathrm{Re}(A) \geq (g - Tk^2/\rho)k\sinh(kH)$.

A graph of $(g - Tk^2/\rho)k\sinh(kH)$ against k is shown in Figure 2. It is worth noting that, in the absence of any control input (i.e. $A = 0$), c is purely real and the system is stable when the $(g - Tk^2/\rho)$ term is positive. This corresponds to surface tension effects being larger than gravitational effects. Conversely, c is purely imaginary and the system is unstable when $(g - Tk^2/\rho)$ is negative. Note that the $k\sinh(kH)$ factor is always positive.

The graph is seen to have two distinct maxima, which implies that if the constant A is chosen to be sufficiently large, instability is prevented for all wavelengths. It is interesting to note that $Z = A/\omega^2$ implies that $\omega^2\hat{\varepsilon}(k, \omega) = A\hat{\eta}(k, \omega)$. Hence, this form of transfer function is equivalent to controlling the vertical acceleration of the surface at $y = H$ to mimic the interface displacement, not one would think an impossible task if the necessary distributed actuators were available.

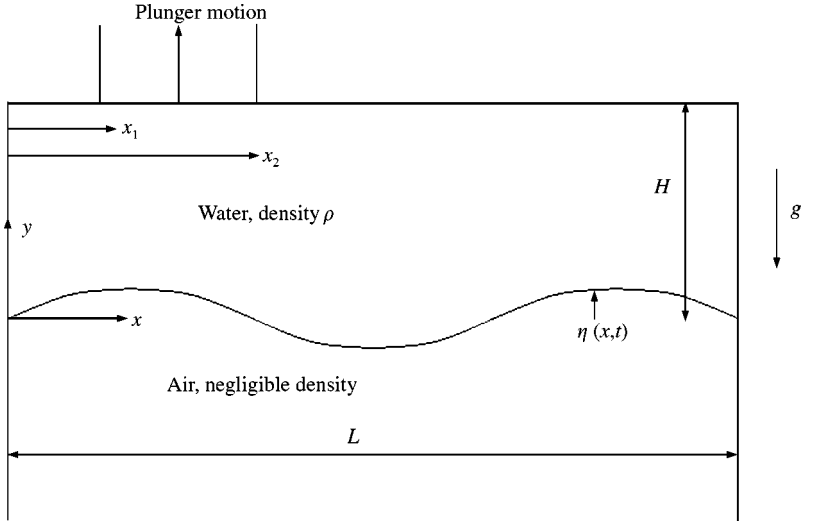

Figure 3. The confined layer of water.

3. THE LAYER CONFINED BETWEEN VERTICAL WALLS

A more practical example is provided when the same layer of water is confined between two vertical walls, a distance L apart. The ceiling now contains a single plunger whose vertical motion can be controlled; see Figure 3. It is assumed that the displacement of the plunger is so small that the flow it produces is strictly linear.

3.1. Analysis

To account for the effect of the vertical walls, the method of images is used. The correct image system is shown in Figure 4; it is infinite and periodic in x with period $2L$. This suggests the use of the general range Fourier series for $0 \leq x \leq 2L$. Symmetry about $x = 0$ implies that the sine coefficients in the Fourier series for the interface displacement, ceiling velocity and velocity potential will be zero and that only the cosine terms need be considered.

The interface displacement and ceiling velocity can be expressed as the following Fourier series, where the "hat" denotes a Fourier transform,

$$\eta(x, t) = \sum_{n=1}^{\infty} \left\{ \frac{1}{2\pi} \int_{-\infty}^{\infty} \hat{\eta}(n, \omega) e^{i\omega t}\, d\omega \right\} \cos(n\pi x/L), \tag{9}$$

$$v(x, t) = \sum_{n=1}^{\infty} \frac{2[\sin(n\pi x_2/L) - \sin(n\pi x_1/L)]}{\pi n} \left(\frac{1}{2\pi} \int_{-\infty}^{\infty} \hat{v}(\omega) e^{i\omega t}\, d\omega \right) \cos(\pi n x/L). \tag{10}$$

The flow in the water region is incompressible, inviscid and irrotational, and therefore obeys Laplace's equation and the unsteady Bernoulli equation [i.e., equations (3) and (4)].

Force equilibrium at the interface, where $\tilde{p}_1$ is the pressure fluctuation directly above the interface gives

$$-\tilde{p}_1 + T \frac{\partial^2 \eta}{\partial x^2} = 0. \tag{11}$$

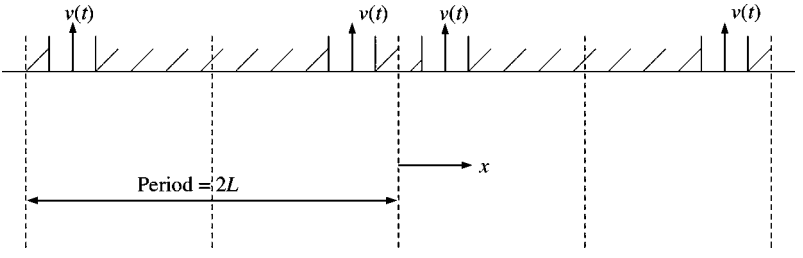

Figure 4. The image system.

The boundary conditions for velocity are

$$\frac{\partial \phi}{\partial y} = \frac{\partial \eta}{\partial t} \quad \text{at } y = \eta \ (\eta \text{ small}) \quad \text{and} \quad \frac{\partial \phi}{\partial y} = v(x, t) \quad \text{at } y = H. \tag{12}$$

Applying equations (3), (4) and (11) and making use of equation (12) gives the following relationship between the plunger velocity and the interface displacement:

$$\hat{\eta}(n, \omega)\left(T\left(\frac{n\pi}{L}\right)^2 - \rho g - \frac{\rho \omega^2 L}{\pi n \tanh(\pi n H/L)}\right) = \hat{v}(\omega)\frac{4\rho L i\omega \mathrm{e}^{-\pi n H/L}[\sin(\pi n x_2/L) - \sin(\pi n x_1/L)]}{\pi^2 n^2 (1 - \mathrm{e}^{-2\pi n H/L})}. \tag{13}$$

This is an important equation. The natural frequencies of the uncontrolled system can be deduced from it by setting $\hat{v}(\omega) = 0$. Ignoring the trivial solution in which there is no disturbance gives the natural frequencies as

$$\omega_n = \pm \sqrt{\frac{\pi n \tanh(\pi n H/L)}{\rho L}\left(T\left(\frac{\pi n}{L}\right)^2 - \rho g\right)}. \tag{14}$$

Instability of a mode is characterised by its natural frequency having a nonzero imaginary part of the correct sign. If the natural frequency is purely real, the corresponding mode is marginally stable. These arguments, combined with equation (14) can be used to translate the requirement that only the first mode is unstable into an allowed range for the channel width L. The allowed range is given in equation (15) and interestingly is independent of water depth, H,

$$\pi \sqrt{\frac{T}{\rho g}} < L < 2\pi \sqrt{\frac{T}{\rho g}}. \tag{15}$$

Note that if the first n modes are required to be unstable then the allowed range for the channel width remains independent of H and becomes,

$$n\pi \sqrt{\frac{T}{\rho g}} < L < (n + 1)\pi \sqrt{\frac{T}{\rho g}}.$$

If it is required that all modes be stable, the restriction on the channel width becomes $L < \pi\sqrt{T/\rho g}$. Hence, in theory, H can be infinitely large and surface tension alone can "hold up" an infinite amount of water!

Some realistic values for the water–air system being considered are $T = 0{\cdot}074\ \mathrm{kg/s^2}$, $\rho = 1000\ \mathrm{kg/m^3}$ and $g = 9{\cdot}81\ \mathrm{m/s^2}$. Substituting these into equation (15) gives the allowed channel width range as being $8{\cdot}6\ \mathrm{mm} < L < 17{\cdot}3\ \mathrm{mm}$. Choosing $L = 14\ \mathrm{mm}$, arbitrarily

setting $x_1 = 3$ mm, $x_2 = 6$ mm, $H = 10$ mm and substituting into equation (7) gives the transfer function from $\hat{v}(\omega)$ to $\hat{\eta}(n, \omega)$ as being

$$\frac{\hat{\eta}(n,\omega)}{\hat{v}(\omega)} = \frac{4\rho_1 \mathrm{i}\omega \mathrm{e}^{-\pi n H/L}[\sin(\pi n x_2/L) - \sin(\pi n x_1/L)]/(\pi^2 n^2(1 - \mathrm{e}^{-2\pi n H/L}))}{T(n\pi/L)^2 - \rho_1 g - \rho_1 \omega^2 L/\pi n \tanh(\pi n H/L)}$$

$$= \frac{60\mathrm{i}\omega \mathrm{e}^{-2{\cdot}094n}[\sin(1{\cdot}257n) - \sin(0{\cdot}628n)]/(\pi^2 n^2(1 - \mathrm{e}^{-4{\cdot}189n}))}{3246n^2 - 9810 - (4{\cdot}775\omega^2)/n \tanh(2{\cdot}094n)}. \quad (16)$$

3.2. Designing a Control System

For a transfer function to be used as the basis of any control system design, it must be between an easily controllable and an easily measurable quantity. Whilst $v(t)$ might be easily controllable, $\eta(n, t)$ is not so easily measurable. In its present form, equation (16) is therefore not a good basis for control system design; further manipulation is required.

Expressing $\hat{\eta}(x, \omega)$ as a Fourier series gives $\hat{\eta}(x, \omega) = \sum_{n=1}^{\infty} \hat{\eta}(n, \omega)\cos(n\pi x/L)$. Hence, the time Fourier transform of the interface displacement at $x = 0$ can be written as

$$\hat{\eta}(x = 0, \omega) = \sum_{n=1}^{\infty} \hat{\eta}(n, \omega) = \hat{\eta}(1, \omega) + \hat{\eta}(2, \omega) + \hat{\eta}(3, \omega) + \cdots$$

Substituting the values of n into equation (10), the transfer function from $\hat{v}(\omega)$ to $\hat{\eta}(x, \omega)$ becomes

$$\frac{\hat{\eta}(x = 0, \omega)}{\hat{v}(\omega)} = \frac{0{\cdot}2138\mathrm{i}\omega}{-6{\cdot}084 - 4{\cdot}558\omega^2} + \frac{-0{\cdot}00863\mathrm{i}\omega}{5095 - 2{\cdot}229\omega^2} + \frac{-0{\cdot}00127\mathrm{i}\omega}{23730 - 1{\cdot}485\omega^2} + \cdots \quad (17)$$

Since the system is causal, it is valid to recast equation (17) in terms of Laplace transforms by setting $s = \mathrm{i}\omega$,

$$\frac{\hat{\eta}(x = 0, s)}{\hat{v}(s)} = \frac{0{\cdot}2138s}{-6{\cdot}084 + 4{\cdot}558s^2} + \frac{-0{\cdot}00863s}{5095 + 2{\cdot}229s^2} + \frac{-0{\cdot}00127s}{23730 + 1{\cdot}485s^2} + \cdots. \quad (18)$$

Now, $\eta(x = 0, t)$ represents the interface displacement at one of the walls and is therefore a measurable property of the system and (18) can be used as the basis for the control system design. Although in its present form it is the sum of an infinite series, it can be seen from equation (16) that the terms quickly become smaller as n increases. This means that it is reasonable to approximate the series by a finite number of terms. Since the design of the control system will be based on this approximated transfer function, it is necessary to include at least those terms which represent unstable modes.

3.2.1. *Modelling only the first mode*

Since only the first mode is unstable, the transfer function can be approximated by just the first term. This transfer function is denoted by $G_1(s)$,

$$G_1(s) = \frac{\hat{\eta}(x = 0, s)}{\hat{v}(s)} = \frac{0{\cdot}2138s}{-6{\cdot}084 + 4{\cdot}558s^2}. \quad (19)$$

The root locus diagram (Franklin *et al.* 1992) for $G_1(s)$ is shown in Figure 5. The right-half-plane pole confirms that the system is naturally unstable.

The control system is shown in Figure 6. From the root locus diagram for $G_1(s)$, it is apparent that an unstable controller is required for closed loop stability. Considering

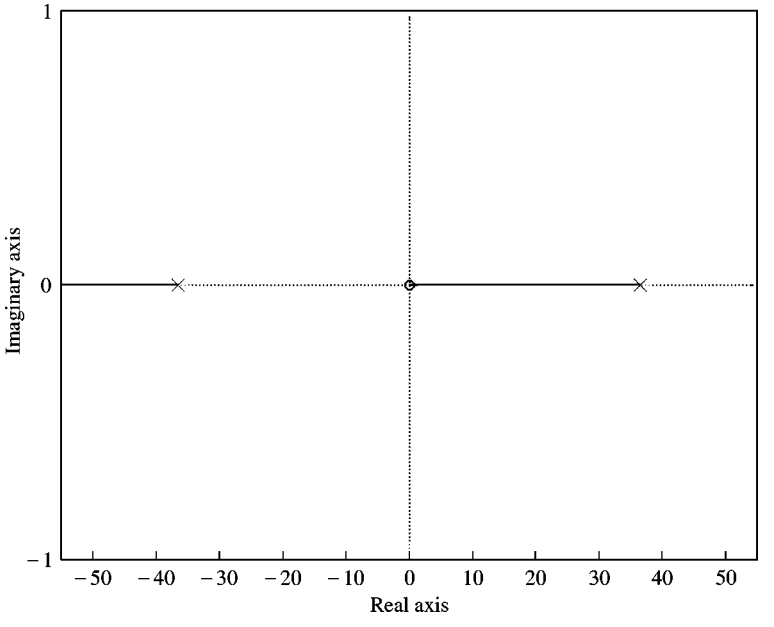

Figure 5. The root locus diagram for $G_1(s)$.

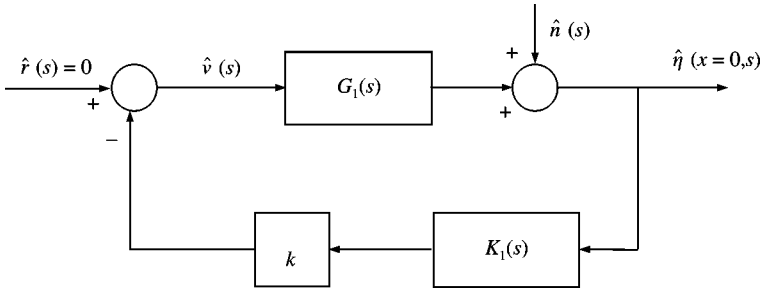

Figure 6. The control system.

a controller of the form $k_1K_1(s) = (as + b)/(s - c)$ and applying the Routh–Hurwitz stability criteria reveals that the closed loop stability will be achieved if $a > 606123$, $b > 28456$ and $c > 0$. An example of a controller which satisfies these criteria is $K_1(s) = (s + 20)/(s - 10)$ with $k_1 = 3000$. The root locus diagram for $G_1(s)K_1(s)$ is shown in Figure 7; it can be seen that $k_1 = 3000$ indeed stabilises the system. The Nyquist diagram for $G_1(s)k_1K_1(s)$ is shown in Figure 8. There are two anti-clockwise encirclements of the -1 point, and there are two unstable open loop poles; this confirms that the closed loop system is stable.

There is a problem with attempting to control the flow in this way, however. Since the plunger velocity is being controlled, a tiny step disturbance, however small, causes the plunger displacement to increase indefinitely. Given that the flow model is based on the assumption that the plunger displacement is small, this is a less than desirable effect. To eliminate this problem, the plunger displacement rather than its velocity should be controlled. The new control system is shown in Figure 9.

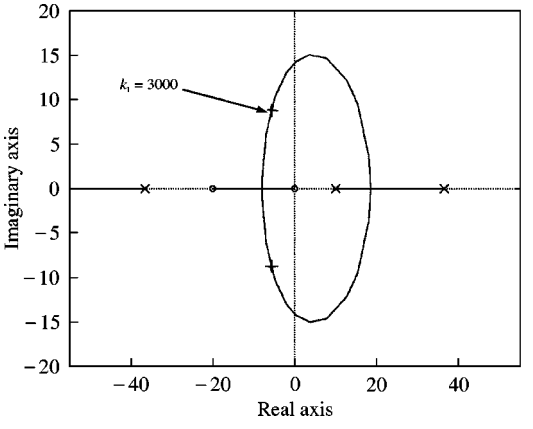

Figure 7. The root locus diagram for $K_1(s)G_1(s)$.

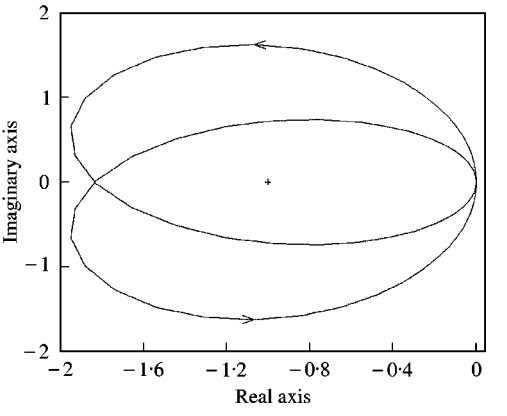

Figure 8. Nyquist diagram for $k_1K_1(s)G_1(s)$.

The root locus for $H_1(s) = sG_1(s)$ is shown in Figure 10. The poles and zeros are identical to those for $G_1(s)$, except for the extra zero at the origin. It is observed that all branches of the plant-controller root locus will have a portion in the left-half plane if the controller consists of two left-half-plane poles near the origin, a right-half-plane pole and two left-half-plane zeros, all appropriately placed. Many controllers can thus achieve stability of the system. However, careful choice of the controller allows the steady state gain from the noise input to the plunger displacement to be minimised, while still ensuring good stability margins. A good compromise is offered by

$$K_1(s) = \frac{(s+27)(s+27)}{(s-35)(s+12)(s+12)} \quad \text{with } k_1 = 2000.$$

Figure 11. shows the root locus diagram for $H_1(s)K_1(s)$.

The motion of the water surface as a function of x and time can be represented using a surface plot. The wall displacement as a function of time is known from the control system and is a sum of contributions from all modes [see equation (20)]. If the contribution from each mode is known, the interface displacement as a function of x can be found using equation (21),

$$\eta(x=0,t) = \sum_{n=1}^{\infty} \eta(n,t), \tag{20}$$

$$\eta(x,t) = \sum_{n=1}^{\infty} \eta(n,t)\cos(n\pi x/L). \tag{21}$$

The contribution decreases with mode number, and so both series can be approximated by just the first term. This means that $\eta(x,t) = \eta(x=0,t)\cos(\pi x/L)$. The surface plot due to a "pulse" input of 10^{-5} m is shown in Figure 12. The "pulse" involves a step of 10^{-5} m at $t = 0$ followed by another step of -10^{-5} m shortly afterwards. The surface plot clearly shows the shape of the first mode, and the fact that the disturbance decays in time.

3.2.2. *Modelling the first three modes*

When the first three terms are included, the transfer function becomes

$$G_2(s) = \frac{\hat{\eta}(x=0,s)}{\hat{v}(s)} = \frac{0{\cdot}2138s}{-6{\cdot}084 + 4{\cdot}558s^2} + \frac{-0{\cdot}00863s}{5095 + 2{\cdot}229s^2} + \frac{-0{\cdot}00127s}{23730 + 1.485s^2}.$$

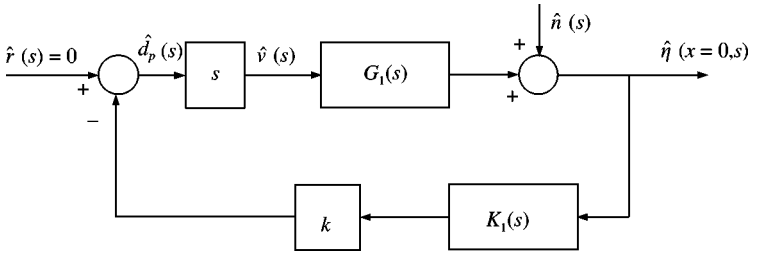

Figure 9. The new control system.

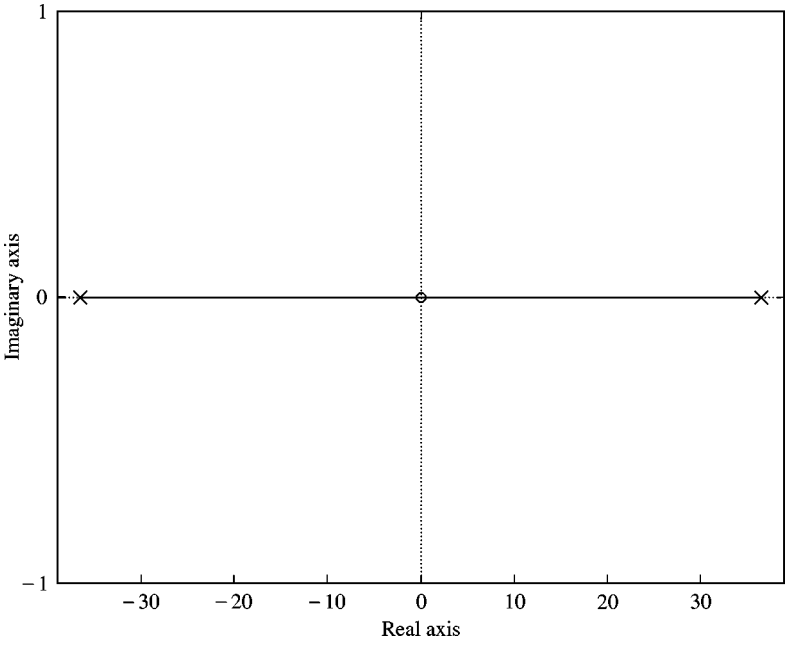

Figure 10. The root locus diagram for $H_1(s)$.

The root locus diagram for $G_2(s)$ is shown in Figure 13 and confirms that the second and third modes are naturally marginally stable. Figure 14 reveals that the control system designed to stabilise the first mode actually destabilises higher modes. In practice, dissipative effects would cause the pole–zero pairs to occur slightly into the left-half plane making destabilisation less likely. However, it is important that there is a way of dealing with this effect.

Extra controllers which place left-half plane pole-zero pairs very close to the existing imaginary axis pairs can be used; they "drag" the root locus branches into the left-half plane, preventing instability. The effect is clearly seen in Figure 15. The extra controllers can be combined with a controller similar to that previously derived. A good design for this system was found to be

$$K_2(s) = \frac{(s^2 + 54s + 729)(s^2 + 0{\cdot}5s + 15700)(s^2 + 0{\cdot}5s + 2250)}{(s^3 - 11s^2 - 696s - 5040)(s^2 + 0{\cdot}5s + 16500)(s^2 + 0{\cdot}5s + 2650)} \quad \text{with } k_2 = 2500.$$

The interface motion due to a "pulse" input is shown in Figure 16. The presence of the closed loop poles near the origin due to the higher modes cause the high frequency oscillations to be superimposed on the main response.

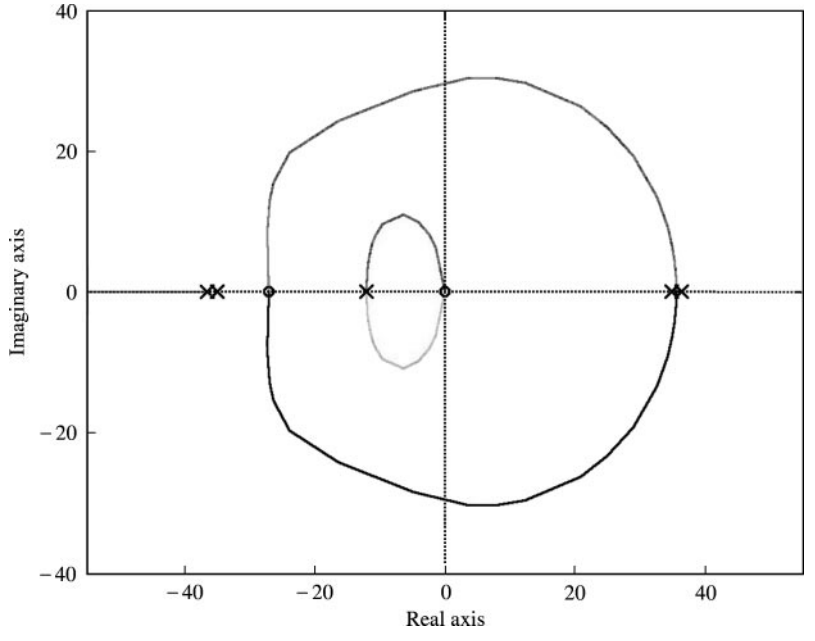

Figure 11. The root locus diagram for $H_1(s)K(s)$.

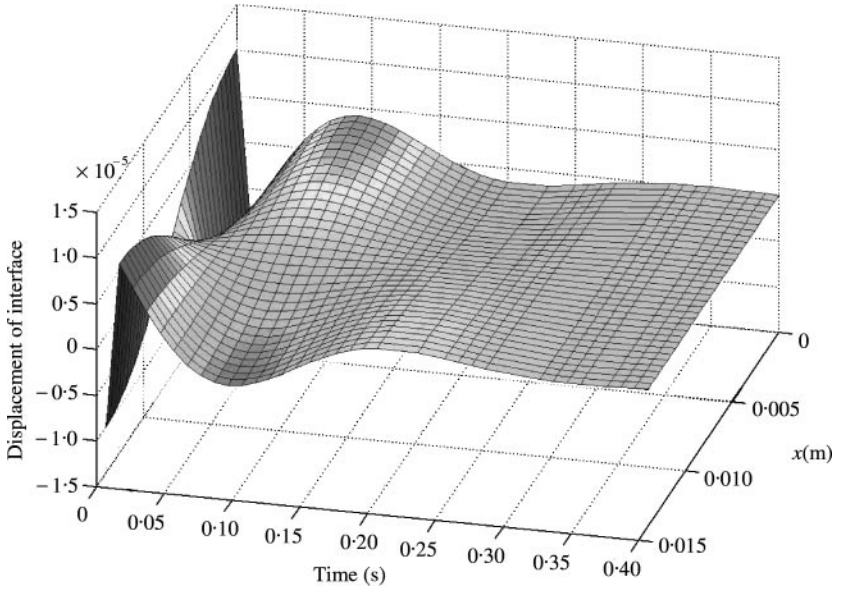

Figure 12. Surface plot for a "pulse" input of 10^{-5} m.

3.2.3. *More than one unstable wavelength*

If the channel width is such that there are two unstable wavelengths, the root locus diagram takes the form shown in Figure 17. There are two right-half-plane poles, and no combination of controller poles and zeros can cause all branches of the combined root locus to have a portion in the left-half plane. The same is found for there being more than two unstable

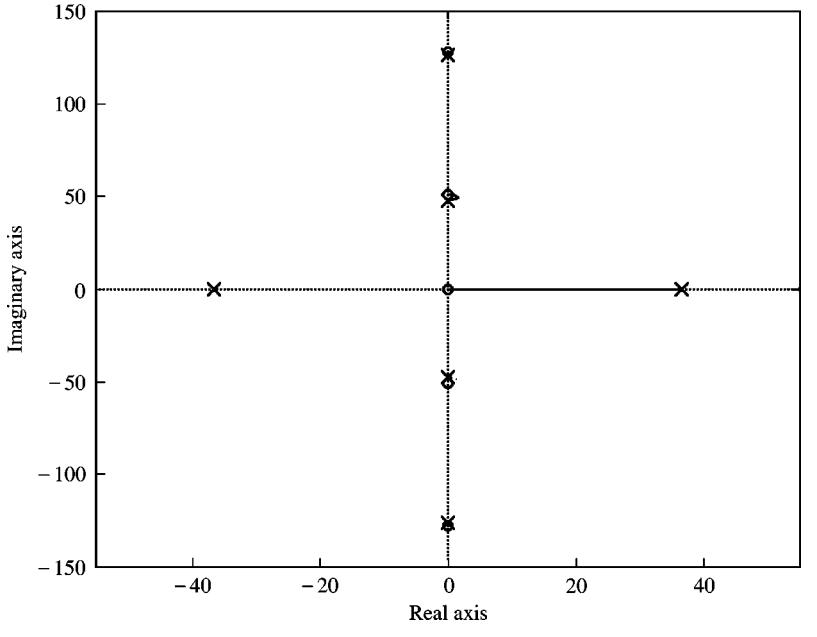

Figure 13. The root locus diagram for $G_2(s)$.

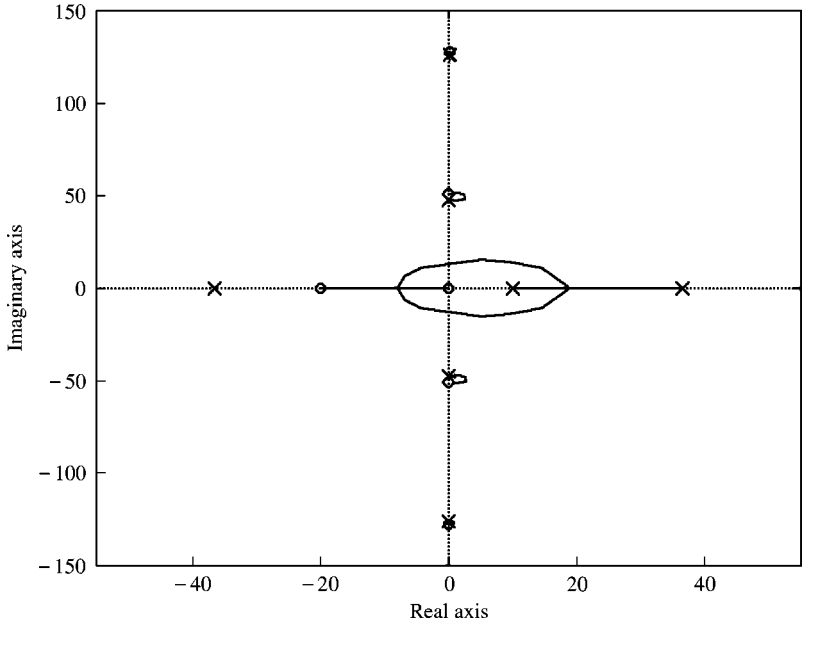

Figure 14. The root locus diagram for $G_2(s)K_1(s)$.

wavelengths. Thus, unsurprisingly, a system with two or more unstable wavelengths cannot be stabilised by controlling the vertical motion of a single plunger. More control actuators would be needed to give more control degrees of freedom. What has been considered in this paper is probably the simplest case, which was the intention for ease of illustration.

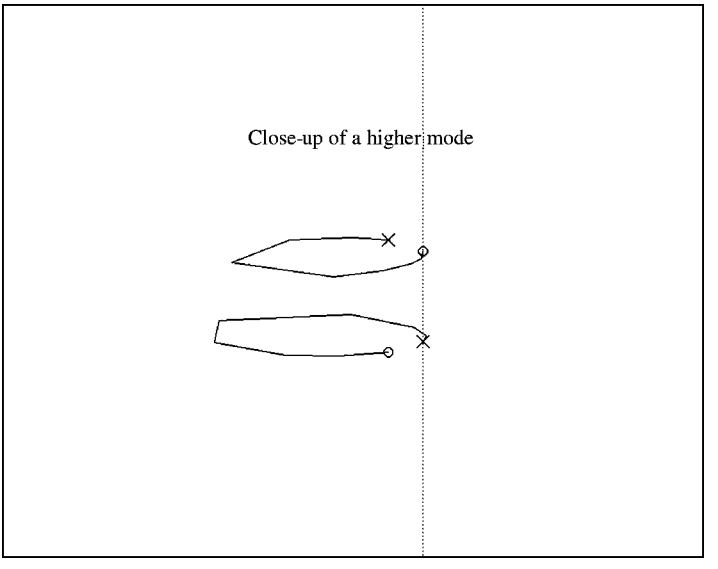

Figure 15. The root locus diagram for $G_2(s)K_2(s)$.

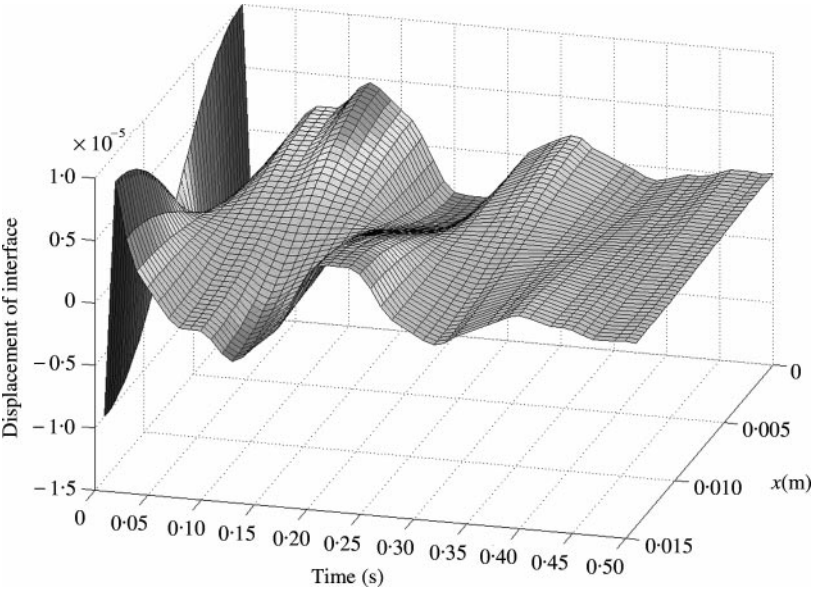

Figure 16. Surface plot for a "pulse" input of 10^{-5} m.

4 CONCLUSIONS

It has been shown that active control can be used to stabilise two specific cases of the negative buoyancy instability. For an unbounded layer of water containing an infinite number of unstable modes, an idealised controller has been identified which would stabilise the system. For a layer confined between two vertical walls in such a way that there is just one naturally unstable wavelength, a simple, realisable controller has been designed which would stabilise this wavelength. Both these cases illustrate that it is possible, and sometimes

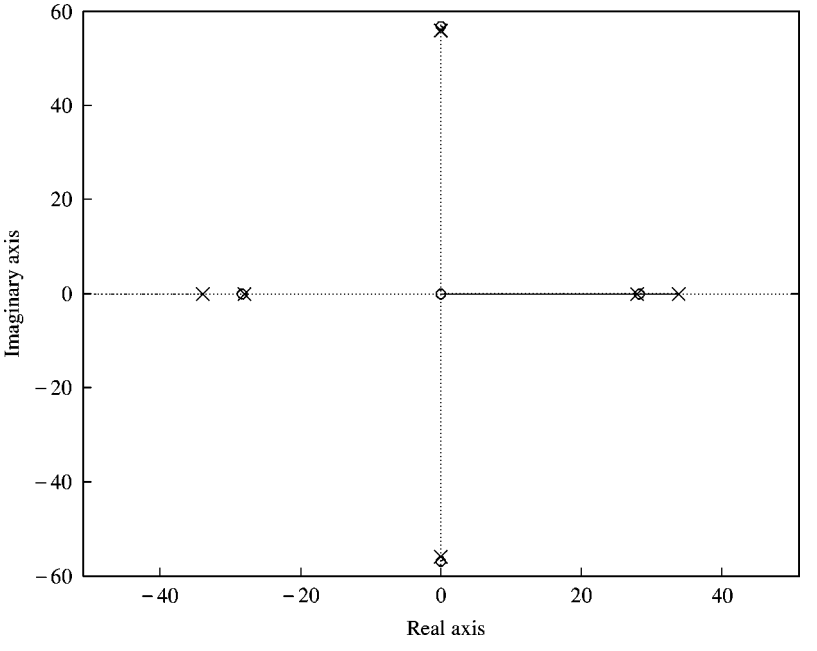

Figure 17. The root locus diagram when there are two unstable modes.

feasible, to retain a layer of water attached to the underside of a ceiling indefinitely. This seemingly unnatural state is brought about because the natural properties of the coupled flow-controller system differ significantly from those of the flow system alone.

References

FFOWCS WILLIAMS, J. E. 1982 Sound sources in aerodynamics — Fact and fiction. *AIAA Journal* **20,** 307–315.

FFOWCS WILLIAMS, J. E. 2001 Active flow control. *Journal of Sound and Vibration* **239,** 861–871.

PEAKE, N. & CRIGHTON, D. G. 2000 Active control of sound. *Annual Review of Fluid Mechanics* **32,** 137–164.

FRANKLIN, G. F., POWELL, J. D. & EMAMI-NAEINI, A. 1994 *Feedback Control of Dynamic Systems.* Reading, MA: Addison Wesley, Chapter 5, pp. 243–336.